Coordination Distortion

DOI: 10.1002/ange.201402339

A Displacive-Type Metal Crown Ether Ferroelectric Compound: $Ca(NO_3)_2$(15-crown-5)**

*Heng-Yun Ye, Yi Zhang, Da-Wei Fu, and Ren-Gen Xiong**

Abstract: *Following the Curie symmetry principle and Aizu rule, we discovered there is a centrosymmetric-to-noncentrosymmetric phase transition in $Ca(NO_3)_2$(15-crown-5) at $T_c = 205$ K. The transition was confirmed by differential scanning calorimetry and second harmonic generation measurements. The transition gives rise to excellent ferroelectricity, such as a giant dielectric anomaly, with faster polarization switching (5×10^{-5} s) of up to 10^7 times without showing fatigue. The ferroelectric mechanism is attributable to the coordination environmental distortion of the central Ca atom. This finding can throw light on the further research in metal–organic ferroelectrics.*

A ferroelectric is a material that undergoes a phase transition from a high-temperature phase (HTP) to a low-temperature phase (LTP); that is, transforming from a linear dielectric to a nonlinear dielectric that has a spontaneous polarization for which the direction can be switched by an applied field.[1] Since the discovery of ferroelectricity in Rochelle salt in 1921 by J. Valasek, numerous applications have been developed, such as non-volatile memory, capacitors, ultrasound imaging and actuators, electro-optic materials for data storage, thermistors, switches known as transchargers or transpolarizers, oscillators and filters, light deflectors, modulators, and displays.[1] However, most commercial ferroelectrics are inorganic ceramics of the perovskite family, such as barium titanate ($BaTiO_3$, BTO) and lead zirconate titanate (Pb{ZrxTi1-x}O_3; PZT), which need high-temperature synthesis and contain environmentally poisonous metals (for example, lead). Thus, there is currently intense research interest among chemists, physicists, and materials scientists in finding new ferroelectrics.[2] Among them, molecular ferroelectrics are the most promising alternatives[3] because they have been shown not only to possess high performance comparable to the inorganic compounds but also have advantages such as light weight, nontoxicity, easy processing, and structural tunability. Although a few new types of molecule-based ferroelectrics, such as perovskite-type metal–organic frameworks,[4] crown-ether-based rotator–stators,[5] and co-crystals based on electronic[6] or hydrogen transfer,[7] have been found in recent years, the search for new ferroelectrics is still a great challenge for scientists.

Ferroelectrics must crystallize in one of the ten polar points groups (C_1, C_s, C_2, C_{2v}, C_3, C_{3v}, C_4, C_{4v}, C_6, C_{6v}) in the ferroelectric phase (below Curie temperature T_c), and may undergo a reversible phase transition abiding by Aizu rule,[8] that is, only 88 species of possible phase transitions, into one of its supergroups, also known as the Curie symmetry principle.[9] Therefore, it is possible to discover potential ferroelectrics by searching Cambridge Crystallographic Data Centre (CCDC) in which numerous polymorphs are recorded for such structures. With this in mind, we noticed a crown-ether metal compound (15-crown-5)bis(nitrato-*O*,*O*′)-calcium(II) (abbreviated as $Ca(NO_3)_2$(15-crown-5)), which meets the requirement (Scheme 1). It crystallizes in a centric space group *Pbca* (D_{2h}) at room temperature, and the lower-temperature structure is in a polar space group $Pna2_1$ (C_{2v}).[10] The low-temperature structure shows a slight coordination environmental distortion of the central calcium atom. We are aware such coordination distortion may be accompanied by novel physical properties, such as spin crossover transitions. Although coordination distortion has also been found to be responsible for ferroelectricity in $BaTiO_3$,[11] in metal–organic compounds, such a mechanism has not been disclosed yet, because the previously reported metal–organic compounds[4,5] are mainly of the order–disorder-type, such as $NaNO_2$,[1] while the displacive mechanism corresponding to the coordination distortion is rare in molecular ferroelectrics. We found the new mechanism in $Ca(NO_3)_2$(15-crown-5) gives rise to high performance in ferroelectricity, such as low-fatigue polarization switching at high frequency. Herein we report the ferroelectric and related physical properties of the first metal–crown-ether complex ferroelectric $Ca(NO_3)_2$(15-crown-5), such as thermal analysis, second harmonic generation (SHG), temperature-dependent dielectric constant, pyroelectricity, and dielectric hysteresis loops.

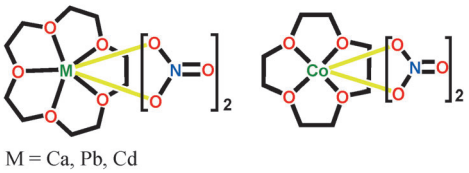

Scheme 1. The structural formula of $M(NO_3)_2$(15-crown-5) (M = Ca (this work), Cd, Pb (Supporting Information)) and $Co(NO_3)_2$(12-crown-4) (Supporting Information).

[*] Dr. H.-Y. Ye, Dr. Y. Zhang, Dr. D.-W. Fu, Prof. R.-G. Xiong
Ordered Matter Science Research Center
Southeast University, Nanjing 211189 (P.R. China)
E-mail: xiongrg@seu.edu.cn

[**] This work was supported by the Project 973 (2014CB848800), the National Natural Science Foundations of China (21290172, 91222101, and 21371032). X.R.G. sincerely thanks Dr. YunYa Liu (Xiangtan University) for his help with fitting Landau coefficients, and the referees for their excellent suggestions.

Supporting information for this article is available on the WWW under http://dx.doi.org/10.1002/anie.201402339.

We first confirmed that there is a structural phase transition between the two temperature structures of Ca-$(NO_3)_2$(15-crown-5) by thermal analysis. The temperature-dependent heat flow in differential scanning calorimetry (DSC) measurement clearly discloses a phase transition at about $T_c = 205$ K (Figure 1). The entropy change (ΔS) is estimated to be about 2.79 J mol^{-1} K^{-1}, which is considerably smaller than $R\ln 2$ (R is the gas constant), indicating not an order–disorder mechanism but rather a displacive mechanism. The shape of peaks and the narrow thermal hysteresis (ca. 2 K) reveal a continuous characteristic, being indicative of a second-order transition.

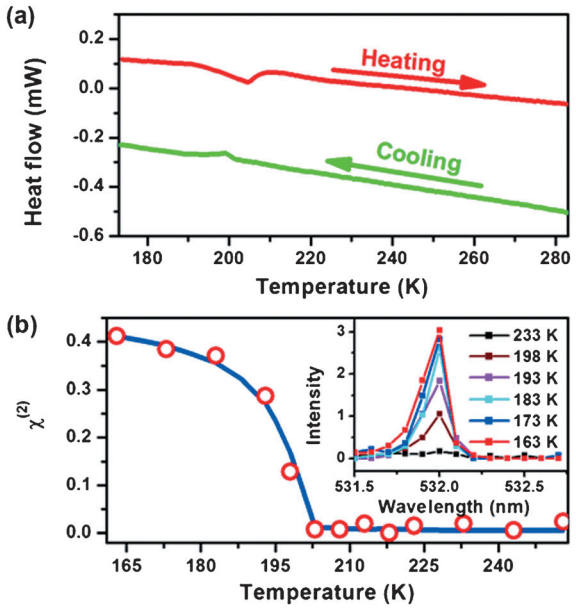

Figure 1. The results of DSC and SHG measurements, revealing a structural phase transition at around $T_c = 205$ K.

To understand the origin of the ferroelectricity through precise structural analysis, we determined a series of structures at different temperatures.[12] The structures in the HTP and LPT are almost identical, respectively. We take the structure determined at 208 K as the average structure of the HTP, and the structure at 93 K as that of the LTP. The HTP is centrosymmetric, space group *Pbca*. The crystal consists of discrete [Ca$(NO_3)_2$(15-crown-5)] molecules (Figure 2a). The Ca ion is nine-coordinate, by a 15-crown-5 and two bidentate nitrate groups. The crown ether is definitely ordered, and its geometry parameters are unexceptional. It chelates the Ca ion with the five O atoms with a perching geometry because of the large diameter of the Ca ion relative to cavity of the crown ether, as observed in other calcium–15-crown-5 systems.[13] The Ca-O_{crown} distances are 2.468(3)–2.582(3) Å, which are comparable to the literature values at room temperature.[10a] The nitrate groups are planar, and the dihedral angle between the two nitrate planes is 75.32(0.12)°. They chelate the Ca ion symmetrically, with differences in Ca–O distances of 0.122(3) and 0.027 Å, respectively, and the O-N-O angles (116.8(3)–122.2(3)°) show a slight deviation

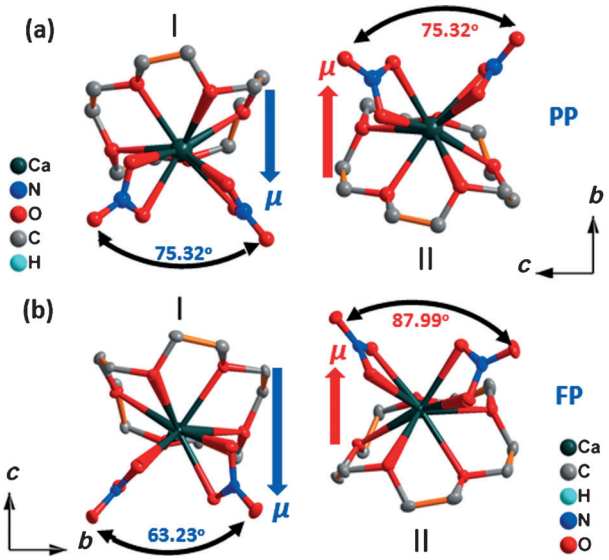

Figure 2. The asymmetric unit of $Ca(NO_3)_2$(15-crown-5) a) in the paraelectric phase (PP) at 208 K, molecule II is generated by the glide symmetry operation of I, and b) in the ferroelectric phase (FP) at 93 K. The dihedral angles between the two nitrate groups are labeled with the curved arrow. The straight arrows indicate the components of the molecular dipole moments in the *c*-direction.

from 120°. The terminal N–O bond is a little shorter than the bridging bonds by ca 0.04 Å.

The LTP assumes a polar space group $Pca2_1$. The relationship between the two temperature cells is $\mathbf{a}^{93k} \approx \mathbf{a}^{208k}$, $\mathbf{b}^{93k} \approx \mathbf{c}^{208k}$ and $\mathbf{c}^{93k} \approx -\mathbf{b}^{208k}$. The structure is refined with a racemic twinning model with the Flack parameter[14] of 0.52(4). The asymmetric unit contains two molecules (Figure 2b). The geometric parameters within the crown ether and the nitrate groups, and the Ca–O distances are comparable to those in the HTP at 208 K. However, the coordination geometries of the central Ca ions show a slight distortion. The dihedral angles between the two nitrate planes are 63.2(10)° and 87.99(10)° for the molecules I and II, respectively. Assuming the positive charges are located on the sites of Ca atoms and the negative charges on the sites of the centers of the nitrate groups, the distortion leads to the change of the distances between the positive and the negative charge from 1.7810 Å in the HTP to 1.82393 Å and 1.73045 Å in the LTP, respectively, and thus unequal dipole moments in the *c*-direction (Figure 2). It appears that the distortion is responsible for the symmetry breaking and occurrence of spontaneous electric polarization (P_s). The estimated P_s is about 0.4 μC cm^{-2}, consistent with the experimental data. The ferroelectric mechanism is illustrated in the Supporting Information, Figure S7.

A check of additional symmetry with PLATON reveals there is a (pseudo) center of symmetry, and the suggested space group is the same as that of the HTP. Therefore, we performed SHG measurement to confirm the centrosymmetric-to-noncentrosymmetric phase transition. As shown in Figure 1b, upon cooling below T_c, [Ca$(NO_3)_2$(15-crown-5)] begins to be SHG-active with a clear peak at 532 nm (frequency doubling), corresponding to the phase transition

from a centrosymmetric structure (*Pbcn*) above T_c to a noncentrosymmetric one ($Pca2_1$) below T_c. $\chi^{(2)}$ in the vicinity of T_c are continuous, also revealing the characteristic of a second-order phase transition. Nevertheless, we still needed evidence from X-ray diffraction. The analysis of the diffraction data reveals a few signs supporting a polar structure. Systematic absence for the twofold screw axis in the *b*-direction ($0k0$, $k = 2n+1$) is unlikely because the $\langle I \rangle$ and $\langle I/\sigma \rangle$ are normal, while in the HTP, they are significantly less than the normal. The mean value of $|E^*E-1|$ of 0.744 is very close to that (0.736) expected for a noncentrosymmetric space group, while in the HTP, it is 0.924, close to that (0.968) expected for a centrosymmetric space group. Although the structure can be solved and refined in the space group *Pbca*, the refinement just converges to $R_1 = 0.23$ and $wR_2 = 0.49$. On the other hand, the existence of pseudo center of symmetry means the low-temperature structure just shows very small difference from that of the HTP. The packing diagrams of the two temperature structures are similar (Supporting Information, Figure S4). This similarity makes the polarization switching possible, that is, the absolute structure can be shifted from one configuration into its crystallograhpically inverted form under an applied electric field.

The ferroelectric nature of the transition is evident from the large dielectric constant anomalies in the *c*-direction at around $T_c = 205$ K. To perform dielectric and other ferroelectric measurements, [001]-direction (relative to the low-temperature structure) unpoled pellets circa 10 mm^2 in area and about 1 mm in the thickness were used. The pellets were cut from single crystals, which were indexed on a Rigaku Satrurn 724^+ diffractometer. The temperature-dependent dielectric constant of $Ca(NO_3)_2$(15-crown-5) is depicted in Figure 3a. The complex dielectric constant ε is defined as $\varepsilon = \varepsilon' - i\varepsilon''$, where ε' and ε'' are the real and imaginary parts of ε, respectively. At low frequencies, ε' reaches a maximum of about 330 at T_c, and the λ-shape peak is indicative of a continuous ferroelectric phase transition. To analyze the characteristic of the phase transition, the temperature dependence of the reciprocal ε' is plotted (the insert of Figure 3a). In the vicinity of T_c, it is linear, obeying Curie–Weiss law, $\varepsilon = \varepsilon_\infty + C/(T-T_0)$. The fitted constant C_{para} of the paraelectric phase ranges from 150 K to 169 K at 500–1 MHz, comparable to those found in colemanite, NH_4HSO_4, $[NH_2CH_2COOH]_2HNO_3$ and $(CH_3NH_3)Al(SO_4)_2{\cdot}12H_2O$ with C_{para} within 2×10^2 K,[15] as well as ($[C_7H_{10}NO$(18-crown-6)$]^+[BF_4]^-$ ($C_7H_{10}NO$ = 4-methoxyanilinium) with $C_{para} = 5\times10^2$ K, and the C_{ferro} of the ferroelectric phase is about 65–99 K (Supporting Information, Table S1). These values are typical of continuous ferroelectric transitions because the ratio of the Curie–Weiss constants C_{para}/C_{ferro} approximates two, as predicted for second-order phase transitions.[16] The extrapolated Curie–Weiss temperature T_0 is in the range of 204.7–205.9 at the frequency range of 500–1000 Hz and very close to T_c determined by DSC, in well agreement with the expectation of Landau theory for a second-order transition. We also measured the dielectric constant along the other non-polar axis. Compared to that in the *c*-direction, the dielectric anomalies are relatively small (Supporting Information, Figure S5).

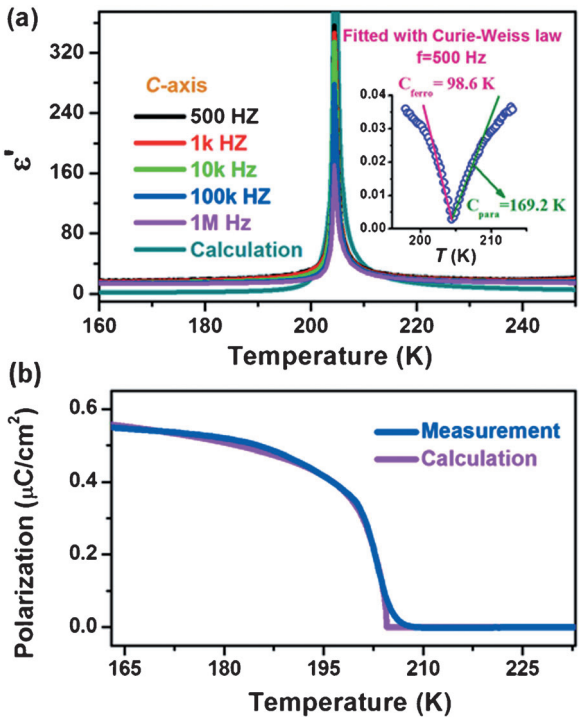

Figure 3. Dielectric and polar response for the transition at 205 K. a) The temperature dependence of the real part of the complex dielectric constant in the *c*-direction. Inset: Plot of $1/\varepsilon'$ versus temperature. b) The temperature dependence of the spontaneous electric polarization P_s calculated by integrating the pyroelectric current upon cooling.

If crystalline materials are ferroelectric, they are definitely pyroelectric. Thus we determined spontaneous polarization through pyroelectric effect. As shown in Figure 3b, P_s is zero above T_c, consistent with the paraelectric behavior, while with temperature decreasing, P_s gradually increase to reach the maximum value 0.55 μC cm^{-2} below T_c. This is slightly larger than those found in Rochelle salt (ca. 0.2 μC cm^{-2}), lithium ammonium tartrate (0.20 μC cm^{-2}), guanidinium aluminum sulfate hexahydrate (0.35 μC cm^{-2}), ammonium sulfate (0.25 μC cm^{-2}), and dicalcium strontium propionate(0.30 μC cm^{-2}),[15] as well as ($[C_7H_{10}NO$(18-crown-6)$]^+[BF_4]^-$ (0.35 μC cm^{-2}),[5a] and comparable to those of colemanite (0.65 μC cm^{-2})[15] and($[C_7H_{10}NO$(18-crown-6)$]^+$-$[ReO_4]^-$ (1.2 μC cm^{-2}),[5b] but significantly smaller than that of triglycine sulphase (TGS; 3.5 μC cm^{-2}).[15] The gradual enhancement instead of a step-like jump indicates that the phase transition should be of second-order, consistent with the results of the DSC, SHG, and dielectric constant measurements.

According to Landau–Devonshire theory, for such a second-order paraelectric-to-ferroelectric phase transition (Aizu notation, *mmmFmm*2), the thermodynamic potential of $Ca(NO_3)_2$(15-crown-5) can be expanded into a polynomial of polarization *P*, and written as the following equation:

$$G = A P^2/2 + B P^4/4 + C P^6/6 + D P^8/8 - PE. \quad (1)$$

Note that all the Landau coefficients are independent of temperature except A. P_s can be determined by minimization of the thermodynamic potential, and the corresponding dielectric constant can be calculated accordingly.[17] The fitted Landau coefficients based on the measured P_s are $A = 5.44(T-204.5) \times 10^8$ m^{2}N/C^2, $B = 2.85 \times 10^{14}$ m^{6}N/C^4, $C = -1.64 \times 10^{19}$ m^{10}N/C^6, and $D = 9.84 \times 10^{23}$ m^{14}N/C^8. The fitted P_s and calculated dielectric constant as functions of temperature are in good agreement with the experimental data, revealing that the transition follows Landau theory.

The ferroelectric polarization switching was confirmed by the measurements of dielectric hysteresis loops (*P-E* loops) on the *c*-plate (001) of single-crystal samples. The results of the *P-E* loops for several temperatures are shown in Figure 4a. Upon cooling, the polarization response is initially

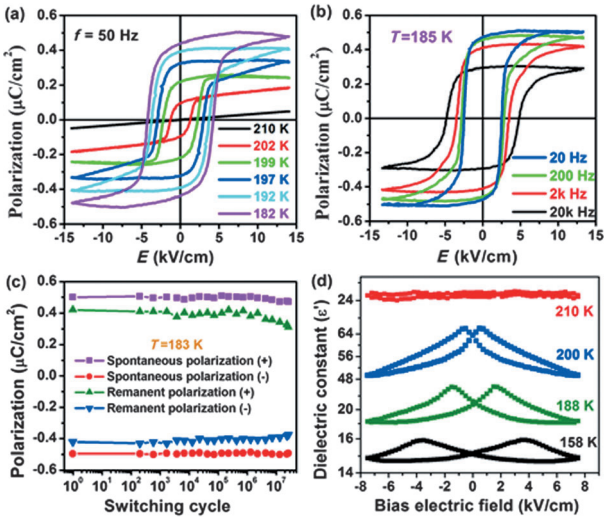

Figure 4. Properties of polarization switching for $Ca(NO_3)_2$(15-crown-5): a) Temperature dependence of *P-E* hysteresis loops at 50 Hz; b) frequency dependence of *P-E* hysteresis loops at 185 K; c) low-fatigue feature measured at 183 K at a frequency of 200 Hz; d) bias field dependence of the complex dielectric constant in both the ferroelectric and the paraelectric phase.

a straight line and no change is seen until 210 K, indicating the status above this temperature is still paraelectric or linearly dielectric. It begins to open and suddenly grows into a small loop at about 202 K below T_c, showing the current status is ferroelectric or nonlinearly dielectric. Upon further cooling, the ferroelectric loops completely open to reach a typical ferroelectric loop at about 182 K. The maximum spontaneous polarization is evaluated to be about 0.50 μC cm^{-2} at 182 K, with remanent polarization of 0.45 μC cm^{-2}, in good agreement with that obtained from the pyroelectricity measurement.

The frequency dependency of polarization switching is the key property for the application such as in non-volatile memory. We thus examined its frequency dependency of P_s (Figure 4b), and found switching time about 5×10^{-5} second is relatively fast, much longer than those found in inorganic perovskites ferroelectrics (a few nanoseconds) but much shorter than those found in pure organic ferroelectrics (about a second)[6] and some polymer materials (about 10^{-3} second).[18] It is interesting to find that even at a high frequency (20 kHz), the *P-E* hysteresis loops retain high rectangularity. The high performance in polarization switching is rare[3a,b] Moreover, a preliminary study on the ferroelectric fatigue properties shows that P_s remains unchanged after 1×10^7 switching operations cycles. This could throw light on further research in applications based on metal–organic FeRAMs.

The revealed nonlinear dielectric dependence on electric field is further verified by directly measuring dielectric constant as a function of the bias electric field (E). As illustrated in Figure 4d, ε' is basically bias-voltage independent and remains a straight line (Figure 4d) above T_c, showing linear dielectric response like that of most ordinary dielectrics. Below T_c, the dependence displays butterfly-shaped curves with mirror symmetry as observed in the typical molecular ferroelectric triglycine sulphase (Supporting Information, Figure S6), corresponding to the polarization switching behavior as revealed in the *P-E* hysteresis loop measurements. Owing to the nonlinearity, such ferroelectric materials might find application in tunable microwave devices, such as electronically tunable mixers, delay lines, filters, and phase shifters.[1]

Interestingly, a preliminary investigation on other similar compounds, including $Cd(NO_3)_2$(15-crown-5),[19] $Pb(NO_3)_2$(15-crown-5), and $Co(NO_3)_2$(12-crown-4) (Supporting Information, Figures S8–S17, Tables S2–S4) reveals they are probably ferroelectric, and the ferroelectric mechanism of $Ca(NO_3)_2$(15-crown-5) also applies to them. The growth of large crystals for systematic characterization is in progress.

In summary, we have discovered a new displacive-type metal–crown-ether ferroelectric $Ca(NO_3)_2$(15-crown-5) using the Curie symmetry principle and Aizu rule based on CCDC. The observed excellent ferroelectricity will throw light on the further research on the exploration of metal–organic complexes as ferroelectric materials. The displacive mechanism, corresponding to the coordination environmental distortion of the central Ca atom, is observed for the first time in molecular ferroelectrics, which would contribute to the deep understanding of the ferroelectric origin in the emerging metal–organic ferroelectrics, and to the search for new ferroelectricity in metal–organic compounds because many physical phenomena, such as spin crossover transitions, are accompanied by coordination distortion.

Experimental Section

The crystals of $Ca(NO_3)_2$(15-crown-5) were obtained by slowing evaporation of an aqueous solution containing stoichiometric $Ca(NO_3)_2$ and 15-crown-5 at room temperature. The purity of the bulk phase was verified by an IR spectrum and powder X-ray diffraction (Supporting Information, Figures S1–S3). Other metal–crown-ether compounds in the Supporting Information were prepared using the same procedure. Variable-temperature X-ray single-crystal diffraction analysis was carried out using a Rigaku Saturn 724$^+$ CCD diffractometer with Mo-Kα radiation ($\lambda = 0.71073$ Å). Data collection, cell refinement, and data reduction was performed using Rigaku CrystalClear 1.3.5. The structures were solved by direct methods and

refined by the full-matrix method based on F^2 using the SHELXTL software package. All non-hydrogen atoms were refined anisotropically and the positions of all hydrogen atoms were generated geometrically. CCDC 986014, 986015, 986016, 986017, 986018, 986019, 986020 (for $Ca(NO_3)_2$(15-crown-5)), 998561, 998562, 9985631, 998564, 998565 (for other metal-ether compounds) contain the supplementary crystallographic data for this paper. These data can be obtained free of charge from The Cambridge Crystallographic Data Centre via www.ccdc.cam.ac.uk/data_request/cif.

X-ray powder diffraction was measured on a Rigaku DMX/2000 X-ray diffraction instrument. DSC measurements were performed using a Rigaku Thermal series instrument with the heating and cooling rate of 10 K min^{-1}. For dielectric measurements, the samples were made with single-crystals cut into the form of thin plates perpendicular to the crystal axes. Silver conductive paste deposited on the surfaces of the plates was used as the electrodes. Complex dielectric permittivity was measured with an Agilent 4284A impedance analyzer at the frequency range from 20 Hz to 1 MHz with an applied electric field of 0.5 V. The *P-E* hysteresis loops were recorded on a Sawyer–Tower circuit, Precision Premier II (Radiant Technologies, Inc.). The ferroelectric fatigue test was performed with the same conditions as in the measurement of the *P-E* hysteresis loop. The dielectric measurements at a frequency of 1 kHz with a DC bias field ranging from −600 V to +600 V were performed using a Novocontrol Alpha-A high-performance frequency analyzer. The temperature dependence of spontaneous polarization was calculated by integrating the pyroelectric current. The pyroelectric current was measured using an electrometer (Keithley 6517B) under zero electric field in a cooling run at a rate of 10 K min^{-1}. For SHG experiments, an unexpanded laser beam with low divergence (pulsed Nd:YAG at a wavelength of 1064 nm, 5 ns pulse duration, 1.6 MW peak power, 10 Hz repetition rate) was used. The instrument model is FLS 920, Edinburgh Instruments and the low temperature system is 10–325 K, DE 202, while the laser is Vibrant 355 II, OPOTEK. The numerical values of the nonlinear optical coefficients for SHG have been determined by comparison with a KDP reference.

Received: February 12, 2014
Published online: May 20, 2014

Keywords: coordination distortion · crown-ether complexes · dielectricity · ferroelectricity · structural phase transitions

[1] M. E. Lines, A. M. Glass, *Principles and Applications of Ferroelectrics and Related Materials*, Oxford University Press, Oxford, **1977**.

[2] a) S. W. Kim, H. Y. Chang, P. S. Halasyamani, *J. Am. Chem. Soc.* **2010**, *132*, 17684 – 17685; b) A. Katrusiak, M. Szafrański, *Phys. Rev. Lett.* **1999**, *82*, 576 – 579; c) W. Zhang, R.-G. Xiong, *Chem. Rev.* **2012**, *112*, 1163 – 1195; d) S. Horiuchi, R. Kumai, Y. Tokunaga, Y. Tokura, *J. Am. Chem. Soc.* **2008**, *130*, 13382 – 13391; e) Y. Zhang, W. Zhang, S.-H. Li, Q. Y, H.-L. Cai, F. Deng, R.-G. Xiong, S. P. D. Huang, *J. Am. Chem. Soc.* **2012**, *134*, 11044 – 11049; f) Z. G. Guo, R. Cao, X. Wang, H. F. Li, W. B. Yuan, G. J. Wang, H. H. Wu, J. Li, *J. Am. Chem. Soc.* **2009**, *131*, 6894 – 6895; g) S. Ohkoshi, H. Tokoro, T. Matsuda, H. Takahashi, H. Irie, K. Hashimoto, *Angew. Chem.* **2007**, *119*, 3302 – 3305; *Angew. Chem. Int. Ed.* **2007**, *46*, 3238 – 3241.

[3] a) D.-W. Fu, H.-L. Cai, Y. M. Liu, Q. Ye, W. Zhang, Y. Zhang, X.-Y. Chen, G. Giovannetti, M. Capone, J. Y. Li, R.-G. Xiong, *Science* **2013**, *339*, 425 – 428; b) H.-L. Cai, W. Zhang, J.-Z. Ge, Y. Zhang, K. Awaga, T. Nakamura, R.-G. Xiong, *Phys. Rev. Lett.* **2011**, *107*, 147601; c) H.-Y. Ye, Y. Zhang, S.-I. Noro, K. Kubo, M. Yoshitake, Z.-Q. Liu, H.-L. Cai, D.-W. Fu, H. Yoshikawa, K. Awaga, R.-G. Xiong, T. Nakamura, *Sci. Rep.* **2013**, *3*, 2249; d) S. Horiuchi, Y. Tokura, *Nat. Mater.* **2008**, *7*, 357 – 366; e) G. Rogez, N. Viart, M. Drillon, *Angew. Chem.* **2010**, *122*, 1965 – 1967; *Angew. Chem. Int. Ed.* **2010**, *49*, 1921 – 1923; f) Z. H. Sun, T. L. Chen, J. H. Luo, M. C. Hong, *Angew. Chem.* **2012**, *124*, 3937 – 3942; *Angew. Chem. Int. Ed.* **2012**, *51*, 3871 – 3876; g) Y. Zhang, Y. Liu, H. Y. Ye, D. W. Fu, W. Gao, H. Ma, Z. Liu, Y. Liu, W. Zhang, J. Li, G. L. Yuan, R. G. Xiong, *Angew. Chem.* **2014**, *126*, 5164 – 5168; *Angew. Chem. Int. Ed.* **2014**, *53*, 5064 – 5068.

[4] a) D. Di Sante, A. Stroppa, P. Jain, S. Picozzi, *J. Am. Chem. Soc.* **2013**, *135*, 18126 – 18130; b) D.-W. Fu, W. Zhang, H.-L. Cai, Y. Zhang, J.-Z. Ge, R.-G. Xiong, S. P. D. Huang, T. Nakamura, *Angew. Chem.* **2010**, *122*, 6758 – 6760; *Angew. Chem. Int. Ed.* **2010**, *49*, 6608 – 6610; c) G.-C. Xu, X.-M. Ma, L. Zhang, Z.-M. Wang, S. Gao, *J. Am. Chem. Soc.* **2010**, *132*, 9588 – 9590; d) P. Jain, V. Ramachandran, R. J. Clark, H. D. Zhou, B. H. Toby, N. S. Dalal, H. W. Kroto, A. K. Cheetham, *J. Am. Chem. Soc.* **2009**, *131*, 13625 – 13627; e) H.-B. Cui, B. Zhou, L.-S. Long, Y. Okano, H. Kobayashi, A. Kobayashi, *Angew. Chem.* **2008**, *120*, 3424 – 3428; *Angew. Chem. Int. Ed.* **2008**, *47*, 3376 – 3380; f) A. Stroppa, P. Jain, P. Barone, M. Marsman, J. M. Perez-Mato, A. K. Cheetham, H. W. Kroto, S. Picozzi, *Angew. Chem.* **2011**, *123*, 5969 – 5972; *Angew. Chem. Int. Ed.* **2011**, *50*, 5847 – 5850; g) Y. Zhang, H. Y. Ye, D. W. Fu, W. Zhang, R. G. Xiong, *Inorg. Chem. Front.* **2014**, *1*, 118 – 123.

[5] a) D.-W. Fu, W. Zhang, H.-L. Cai, Y. Zhang, J.-Z. Ge, R.-G. Xiong, S. P. D. Huang, *J. Am. Chem. Soc.* **2011**, *133*, 12780 – 12786; b) D.-W. Fu, H.-L. Cai, S.-H. Li, Q. Ye, L. Zhou, W. Zhang, Y. Zhang, F. Deng, R.-G. Xiong, *Phys. Rev. Lett.* **2013**, *110*, 257601; c) T. Akutagawa, H. Koshinaka, D. Sato, S. Takeda, S.-I. Noro, H. Takahashi, R. Kumai, Y. Tokura, T. Nakamura, *Nat. Mater.* **2009**, *8*, 342 – 347; d) Y. Zhang, H.-Y. Ye, D.-W. Fu, R.-G. Xiong, *Angew. Chem.* **2014**, *126*, 2146 – 2150; *Angew. Chem. Int. Ed.* **2014**, *53*, 2114 – 2118.

[6] A. S. Tayi, A. K. Shveyd, A. C.-H. Sue, J. M. Szarko, B. S. Rolczynski, D. Cao, T. JacksonKennedy, A. A. Sarjeant, C. L. Stern, W. F. Paxton, W. Wu, S. K. Dey, A. C. Fahrenbach, J. R. Guest, H. Mohseni, L. X. Chen, K. L. Wang, J. F. Stoddart, S. I. Stupp, *Nature* **2012**, *488*, 485 – 489.

[7] a) S. Horiuchi, R. Kumai, Y. Tokura, *J. Am. Chem. Soc.* **2013**, *135*, 4492 – 4500; b) S. Horiuchi, R. Kumai, Y. Tokura, *Angew. Chem.* **2007**, *119*, 3567 – 3571; *Angew. Chem. Int. Ed.* **2007**, *46*, 3497 – 3501.

[8] K. Aizu, *J. Phys. Soc. Jpn.* **1969**, *27*, 387 – 396.

[9] I. S. Zheludev in *Solid State Physics*, *Vol. 26* (Eds.: H. Ehrenreich, F. Seitz, D. Turnbull), Academic Press, New York, **1971**, pp. 429 – 464.

[10] a) P. C. Junk, J. W. Steed, *J. Chem. Soc. Dalton Trans.* **1999**, 407 – 414; b) M. D. Brown, W. Levason, M. Webster, *Acta Crystallogr. Sect. E* **2005**, *61*, m1015-m1017.

[11] a) K. H. Weyrich, *Ferroelectrics* **1990**, *104*, 183 – 194; b) K. H. Weyrich, P. Madenach, *Ferroelectrics* **1990**, *111*, 9 – 14.

[12] Crystal data for $Ca(NO_3)_2$(15-crown-5) at 373 K: $M_r = 384.36$, orthorhombic, *Pbca*, $a = 15.310(8)$, $b = 13.660(7)$, $c = 16.168(8)$ Å, $V = 3381(3)$ Å^3, $Z = 8$, $\rho_{calcd} = 1.510$ g cm^{-3}, R_1 ($I > 2\sigma(I)$) = 0.0685, wR_2 (all data) = 0.1494, $m = 0.429$ mm^{-1}, $S = 1.153$. At 323 K: orthorhombic, *Pbca*, $a = 15.232(5)$, $b = 13.532(7)$, $c = 16.077(8)$ Å, $V = 3320(3)$ Å^3, $Z = 8$, $\rho_{calcd} = 1.538$ g cm^{-3}, R_1 ($I > 2\sigma(I)$) = 0.0604, wR_2 (all data) = 0.1255, $m = 0.437$ mm^{-1}, $S = 1.242$. At 293 K: orthorhombic, *Pbca*, $a = 15.250(6)$, $b = 13.511(5)$, $c = 16.078(6)$ Å, $V = 3313(2)$ Å^3, $Z = 8$, $\rho_{calcd} = 1.541$ g cm^{-3}, R_1 ($I > 2\sigma(I)$) = 0.0739, wR_2 (all data) = 0.1553, $m = 0.438$ mm^{-1}, $S = 1.315$. At 223 K: orthorhombic, *Pbca*, $a = 15.2198(11)$, $b = 13.3689(13)$, $c = 15.9745(15)$ Å, $V = 3250.4(5)$ Å^3, $Z = 8$, $\rho_{calcd} = 1.571$ g cm^{-3}, R_1 ($I > 2\sigma(I)$) = 0.0448, wR_2 (all data) = 0.1015, $m = 0.447$ mm^{-1}, $S = 1.211$. At 208 K: orthorhombic, *Pbca*, $a = 15.232(5)$, $b = 13.373(4)$, $c = 15.993(5)$ Å, $V = 3257.7(19)$ Å^3, $Z = 8$, $\rho_{calcd} = 1.567$ g cm^{-3}, R_1 ($I > 2\sigma(I)$) = 0.0656, wR_2 (all data) = 0.1825, $m = 0.446$ mm^{-1},

$S = 1.380$. At 173 K: orthorhombic, $Pca2_1$, $a = 15.2101(9)$, $b = 15.9269(11)$, $c = 13.2898(10)$ Å, $V = 3219.5(4)$ Å^3, $Z = 8$, $\rho_{calcd} = 1.586\ g\,cm^{-3}$, $R_1\ (I > 2\sigma(I)) = 0.0328$, wR_2 (all data) $= 0.0718$, $m = 0.451\ mm^{-1}$, $S = 1.056$. At 93 K: orthorhombic, $Pca2_1$, $a = 15.233(5)$, $b = 15.899(5)$, $c = 13.221(4)$ Å, $V = 3201.9(18)$ Å^3, $Z = 8$, $\rho_{calcd} = 1.595\ g\,cm^{-3}$, $R_1\ (I > 2\sigma(I)) = 0.0392$, wR_2 (all data) $= 0.0981$, $m = 0.453\ mm^{-1}$, $S = 1.127$.

[13] a) P. C. Junk, J. W. Steed, *J. Coord. Chem.* **2007**, *60*, 1017 – 1021; b) T. S. Pochekutova, V. K. Khamylov, G. K. Fukin, Y. A. Kurskii, B. I. Petrov, A. S. Shavyrin, A. V. Arapova, *Polyhedron* **2011**, *30*, 1945 – 1952; c) Y. Y. Wei, B. Tinant, J.-P. Declercq, M. V. Meerssche, J. Dale, *Acta crystallogr. Sect. C* **1988**, *44*, 73 – 77.

[14] H. D. Flack, *Acta Crystallogr. Sect. A* **1983**, *39*, 876 – 881.

[15] F. Jona, G. Shirane, *Ferroelectric crystals*, Pergamon, Oxford, **1962**.

[16] D. A. Draegert, S. Singh, *Solid state commun.* **1971**, *9*, 595 – 597.

[17] K. M. Rabe, C. H. Ahn, *Physics of Ferroelectrics: A Modern Perspective*, Springer, Berlin, **2007**.

[18] T. Furukawa, *Phase Transitions* **1989**, *18*, 143 – 211.

[19] A. H. Bond, R. D. Rogers, *J. Chem. Crystallogr.* **1998**, *28*, 521 – 527.

